

Article

Seasonal Photosynthetic Activity in the Crown Compartments of European Ash (*Fraxinus excelsior*)

Robert Stanislaw Majewski ¹, Miloš Barták ² , Jan Weger ³, Jan Čermák ¹ and Josef Urban ^{1,*} 

¹ Department of Forest Botany, Dendrology and Geobiocenology, Faculty of Forestry and Wood Technology, Mendel University in Brno, Zemedelská 3, 61300 Brno, Czech Republic

² Department of Experimental Biology, Laboratory of Photosynthetic Processes, Faculty of Science, Masaryk University, Kamenice 5, 62500 Brno, Czech Republic

³ Department of Phytoenergy, Silva Tarouca Research Institute for Landscape and Ornamental Gardening, Public Research Institute, Květnové Náměstí 391, 25243 Průhonice, Czech Republic

* Correspondence: josef.urban@mendelu.cz

Abstract: Leaves facing different directions (north, south, east, and west) receive differing levels of illumination, resulting in spatial differences in photosynthesis P_N in the crowns of mature trees. We measured diurnal trends in P_N for a semi-solitary European ash (*Fraxinus excelsior*) over spring, summer, and autumn and compared these data with leaf biometric traits and leaf area distribution. The highest light-saturated P_N (P_{Nmax}) was to the south and west, and the lowest to the north. Likewise, intrinsic water use efficiency, defined as the ratio ($P_N:g_S$) of photosynthetic rate (P_N) and stomatal conductance (g_S), was also lowest to the north. The thickest leaves were found on the northern face and the thinnest in the south, suggesting differences in leaf anatomy may have contributed to differences in P_N . The greatest leaf area was recorded in the southern crown quadrant, which contributed more than 50% of the tree's accumulated P_N . Our research emphasises the importance of choosing representative leaves for gas exchange measurements. In-depth studies into the spatial distribution of leaves and their traits will be necessary for accurate upscaling of leaf-level photosynthesis to whole tree and canopy levels.

Keywords: net photosynthesis; transpiration; photosynthesis up-scaling; leaf area distribution



Citation: Majewski, R.S.; Barták, M.; Weger, J.; Čermák, J.; Urban, J. Seasonal Photosynthetic Activity in the Crown Compartments of European Ash (*Fraxinus excelsior*). *Forests* **2024**, *15*, 699. <https://doi.org/10.3390/f15040699>

Academic Editor: Nan Xu

Received: 10 March 2024

Revised: 29 March 2024

Accepted: 4 April 2024

Published: 15 April 2024



Copyright: © 2024 by the authors. Licensee MDPI, Basel, Switzerland. This article is an open access article distributed under the terms and conditions of the Creative Commons Attribution (CC BY) license (<https://creativecommons.org/licenses/by/4.0/>).

1. Introduction

Canopy photosynthesis is the primary driver for plant growth and biomass production in numerous ecosystems, including forest stands [1]. However, photosynthesis is commonly measured at the leaf level, and upscaling from leaf level to tree and/or canopy level can present a significant challenge [2]. Of particular importance is canopy heterogeneity, e.g., tree dimensions, differently aged and developed foliage, 3D arrangement of shoots and leaves within the canopy [3], and the dependence of photosynthesis on variations in environmental conditions, e.g., temperature, radiation, or vapour pressure deficit (VPD), whether diurnally or within the canopy. The structure of the canopy will also influence local environmental conditions, providing crucial feedback between structure, environment, and growth. Several studies have shown that canopy structure can affect the absorption of photosynthetically active radiation (PAR), whether in the crown or its compartments, in both broadleaf [4] and coniferous species [5]. In other words, canopy structure and the 3D arrangement of its components can affect both the potential and actual rate of photosynthesis in particular crown compartments. Several 3D canopy architecture models have been developed to evaluate the relationship between canopy compartments and short- and long-term variations in intra-canopy microclimate, light interception, rate of transpiration, and carbon assimilation [6,7]. In solitary and semi-solitary trees, the foliage in different crown compartments may comprise different phenotypes to address environmental gradients that are heterogeneous in space and time [8]. This distinct expression of leaf phenotypes

between crown compartments could lead to complementary patterns in light interception, photosynthesis, and production capacity. For example, Granado-Yela et al. (2011) identified temporal disparity between crown compartments in solitary European olive trees (*Olea europaea*) derived from functional specialisation in photosynthetic behaviour at different functional and spatial scales, i.e., architectural structure (crown level) and carbon budget (leaf level). The same authors also reported differences in photosynthetic rate in leaves from different crown compartments, both in the actual rate of photosynthesis controlled by incident *PAR* and parameters derived from photosynthetic light-response curves [9].

The European ash *Fraxinus excelsior* is frequently found as a semi-solitary tree, and, consequently, optimisation of photosynthetic rates within the species' canopy and its compartments may represent an important aspect of its growth and production strategy. In recent years, in situ measurements alongside modelling approaches have been used to assess within-canopy variation in *PAR* absorption, transpiration, and photosynthesis in solitary trees [10]. To date, however, net photosynthesis in *F. excelsior* has only been studied to a limited extent, with only fragmentary studies on seedlings, e.g., [11,12], while knowledge on photosynthetic rates as affected by leaf category (sun, semi-shade, shade), age, or intra-canopy microclimate remains missing. It is now well-established that maximum net photosynthetic rate (P_{Nmax}) is species-specific within the *Fraxinus* genus, with previous studies reporting a wide range, e.g., the south European flowering ash *F. ornus* 8.0 $\mu\text{mol}(\text{CO}_2)\text{ m}^{-2}\text{ s}^{-1}$ [13], *F. excelsior* 3.8 $\mu\text{mol}(\text{CO}_2)\text{ m}^{-2}\text{ s}^{-1}$ [14], *F. excelsior* 18.0 $\mu\text{mol}(\text{CO}_2)\text{ m}^{-2}\text{ s}^{-1}$ [15], *F. excelsior*—seedlings 12.26 $\mu\text{mol}(\text{CO}_2)\text{ m}^{-2}\text{ s}^{-1}$ [16], American ash *F. americana* 20.0–30.0 $\mu\text{mol}(\text{CO}_2)\text{ m}^{-2}\text{ s}^{-1}$ [17], East-Asian ash *F. rhynchophylla* 8.0 $\mu\text{mol}(\text{CO}_2)\text{ m}^{-2}\text{ s}^{-1}$ [18] and green ash *F. pennsylvanica* 14.6 $\mu\text{mol}(\text{CO}_2)\text{ m}^{-2}\text{ s}^{-1}$ [19].

Likewise, there have been differences reported in net photosynthesis between sun and shade leaves [20], though some other studies have reported no substantial difference, as was the case for *F. ornus* seedlings [21]. In solitary trees, such as the kermes oak *Quercus coccifera* [22], foliage on the outer crown surface (the envelope) facing east, south, or west is considered sun leaf. The sun leaves of broadleaf tree species tend to be smaller and thicker [23] and to have higher photosynthetic rates per unit leaf area than shade leaves [24]. Another ash species, *F. ornus*, exhibits environmental plasticity in leaf structure (leaf mass per area (*LMA*), bulk tissue density, and thickness), which, in solitary trees, results in a markedly higher quantum yield in sun leaves than shade leaves [25]. It has been suggested that degree of shading may play an important role in such cases, with *LMA* in a moderately shaded *F. pennsylvanica*, for example, decreasing only slightly compared to an unshaded control, whereas shoot length and total leaf area increased significantly [26]. As such, variations in photosynthetic response and leaf architecture may be observed, depending on the degree of self-shading on the northern side of solitary trees (*Fraxinus*).

In general, the light environment within a solitary tree crown will be heterogeneous due to both a self-shading effect and the amount of incident light, determined by the elevation of the sun and the azimuth direction of incident light [27]. Consequently, photosynthesis and transpiration in foliage located within the crown will be controlled by both available light at a distinct point and microclimate drivers, such as air temperature and humidity. Nevertheless, our knowledge of how different crown compartments in solitary or semi-solitary *Fraxinus* respond photosynthetically to diel changes in *PAR*, temperature differences, and co-acting environmental factors remains very limited.

The main aim of this study was to perform a series of ecophysiological measurements in a solitary *F. excelsior* and evaluate variations in net photosynthetic activity in differently oriented (north, south, east, and west) crown compartments. Gas exchange measurements were used to evaluate diurnal and seasonal dynamics in P_N and transpiration within the tree canopy. Finally, we describe leaf area distribution and leaf morphology in relation to tree orientation. In doing so, we test the hypothesis that, on days of full sunshine, P_{Nmax} will be highest in east- and south-facing compartments due to leaf acclimation to direct sunshine and light-driven microclimatic parameters. We also hypothesise that the east- and south-facing compartments will contribute most to total carbon assimilation throughout the

day. Finally, we hypothesise that leaf thickness and *LMA* will be lowest in the north-facing crown compartment.

2. Material and Methods

2.1. Site Description

This research took place at the 23 ha Michovky experimental tree nursery (VUKOZ Průhonice, Czech Republic; 49.9919031 N, 14.5765778 E), which was planted in 2004 with a range of experimental tree plots, comprising maples (*Acer* spp.), linden (*Tilia cordata*, *Fraxinus* spp.), rowan (*Sorbus aucuparia*), and Turkish hazel (*Corylus colurna*). Local climate data (precipitation, air temperature and humidity, and soil temperature and soil humidity at different depths) have been collected every 10 min. since 1997 at the Fiedler-Mágr automatic meteorological station, located ca. 100 m from the nursery. *VPD* was calculated from these data using the method outlined in [28].

The local soil is classified as Haplic Luvisol [29], with a higher content of loess in the upper soil layers, giving the soil a distinct heavy character. For a more detailed analysis of soil parameters, see [30]. The nursery understory was originally overgrown with an expansive lawn of native bush reed grass, *Calamagrostis epigejos*, though more recent intensive lawn management (weeding and removal of some trees) has resulted in a more varied plant species pool comprising 93 species, 44 of which are non-native and 13 classified as invasive. Understory conditions depend on season and soil water condition, with dry patches evident during hot and dry periods (from late spring to early autumn), especially on sunny exposures, and extensive moss growth (e.g., *Brachythecium* sp., *Calliergonella cuspidate*, *Oxyrrhynchium hians*) during the wet autumn–winter season. The most common grasses in the spring–summer seasons include common meadow grass (*Poa pratensis*), bush reed, and common mouse-ear chickweed (*Cerastium holosteoides*).

2.2. Experimental Trees and Measuring Periods

A 14-year-old, semi-solitary *F. excelsior*, 8.2 m high and 151 mm in diameter (DBH, $d_{1,3}$), growing at the southern edge of the nursery was selected for experimental measurements (Figure 1).



Figure 1. The 14-year-old nursery plantation at the Michovka research station. The semi-solitary European ash monitored in this study is in the middle-right of the picture. Picture taken from the south-west.

Experimental monitoring took place over three periods in 2017, each representing a different part of the vegetation season. The first measurements were undertaken in late spring (after full leaf canopy development) between 7 and 10 June, the second in summer between 23 and 29 July, and the final measurements in autumn between 27 September and 5 October.

2.3. Gas Exchange Measurements

Measurements of net photosynthesis took place in situ using a portable open-system LiCor-6400XT infrared gas analyser (Li-Cor, Inc., Lincoln, NE, USA) equipped with a transparent leaf chamber, with settings as follows: CO₂ mixer adjusted to natural CO₂ concentration before each measurement—varying between 385 μmol (CO₂) mol (air)⁻¹ and 405 μmol (CO₂) mol (air)⁻¹; flow controller set for 500 μmol s⁻¹ before each measurement; temperature and air humidity left unregulated to be as close to the surrounding environment as possible.

Each hour, a random leaf was selected from the edge and bottom crown sections from the four cardinal directions (north, south, east, and west) and measured. Five points were recorded on each leaf to improve accuracy and for statistical representation, meaning that 20 measurement points were taken each hour. As the whole period from morning to evening was covered, this means that a different number of points are measured each day over the whole measurement period due to changes in day length. Daily trends in net photosynthesis activity (P_N) were selected for the most representative sunny days over each measuring period (i.e., 8 June, 28 July, and 1 October), with the following measuring intervals: 9.5, 9, and 6.3 h, respectively.

2.4. Biometric Measurements

As a first step, crown length in the cardinal and inter-cardinal directions was measured from ground level using a geodetic tape measure. In October, all leaves from the tree crown were collected during an afternoon with total cloud coverage. Then, each branch was cut and wrapped in a waterproof plastic bag for immediate transport to the laboratory for further measurement. At the time of collection, the tree's DBH and height were measured, along with the horizontal angle (azimuth) of each branch and the stem diameter at the height of each branch, to place the branch in Cartesian dimensions.

After collection, three leaf morphology characteristics were measured. First, we measured the total leaf area for each of the four geographic quadrants using a Leaf Area scanner (Masaryk University in Brno, Czech Republic) linked with a computer-calculated leaf area based on the contrast difference between shaded areas of the leaf and background. Next, three representative leaf samples from the two crown levels in each geographic quadrant were collected and transported to the laboratory, where we measured fresh mass and leaf area (as average with no variation) and dry mass after 12 h of drying at 105 °C. Prior to drying, the leaf thickness was measured using digital optical microscopy. First, the fresh leaves were cut to obtain a cross section across the widest part of the leaf blade. The cross-sections were then placed on a glass plate and observed under a VHX-5000 digital microscope with a maximum resolution of 18 megapixels (Keyence, Japan). Images of representative sections were then used to measure the leaf thickness (typically as 10 replicates for each cross section, performed for ca. 15 leaves in each crown compartment) using the linear distance measurements routine in the inbuilt Keyence software package (Keyence, Ver.1.7.0.4, 2014). In total, 150 measurements were taken for each leaf category, i.e., sun and semi-shade.

2.5. Physiological Data Processing

Based on the gas-exchange measurements, values for stomatal conductance (g_s) and P_N were recorded for each geographic canopy compartment (north, east, south, and west) by averaging five independent measurements per canopy compartment and time. From the daily trends obtained, we selected those measured on days of full sun or minimum cloud

cover limiting solar radiation to provide representative days for each measuring period and daily g_S and P_N trends for each azimuthal canopy compartment. The relationship between g_S and P_N for each representative day was then calculated. All P_N data measured in June and July ($n = 112$ for each azimuth direction) were plotted against PAR at the time of measurement, as recorded by the LiCor sensor.

2.6. Statistical Analysis

After confirming the normality of the data using the Shapiro–Wilk test, a one-way ANOVA with the least significant difference test, followed by post hoc Tukey HSC tests, was used to assess differences in photosynthetic parameters. Where the normality test failed (e.g., analysis of leaf thickness), Kruskal–Wallis ANOVA on Ranks with subsequent pairwise multiple comparison procedures (Dunn’s Method) was used instead. All tests were carried out using SigmaPlot v.12.5 at a significance level of $p < 0.05$.

To construct P_N light-response curves, we first fitted a single rectangular hyperbola with three parameters to the data using SigmaPlot v.12.5. Equation coefficients were then estimated for the four geographic points and their standard errors compared by one-way ANOVA and post hoc Tukey HSC tests.

$$P_N = R_d + \frac{P_{Nmax} * PAR}{KI + PAR} \quad (1)$$

By using the single-rectangular hyperbola, we were able to interpret the following coefficients of the model in a physiologically meaningful way:

P_N : net photosynthesis;

R_d : dark respiration;

P_{Nmax} : maximum potential photosynthetic rate per individual;

PAR : a given light intensity measured by LiCor 6400 at leaf level;

KI : half-saturation constant; the light intensity at which the photosynthetic rate proceeds at $\frac{1}{2} P_{Nmax}$.

The following linear trapezoidal method [31] was used to integrate photosynthetic carbon gain over the course of a day:

$$\int_a^b f(x)dx \approx \frac{P_{N2} - P_{N1}}{2} \{P_N(N1) + P_N(N2)\} \quad (2)$$

P_{N2} : subsequent time point of net photosynthesis;

P_{N1} : preceding time point of net photosynthesis.

The composite trapezoidal rule, applied to consecutive intervals, provided an approximate sum for the whole function. We used this method to calculate the accumulated P_N for the different crown compartments over selected days.

3. Results

3.1. Microclimate

The long-term (1997–2017) mean daily temperature at the site was 9.41 °C and the annual sum of precipitation was 548 mm (Figure 2A), while in 2017, the mean daily temperature was 9.9 °C and the annual sum of precipitation was 533 mm (Figure 2B). The highest PAR was recorded on 8 June 2017, when values reached 1756 $\mu\text{mol m}^{-2} \text{s}^{-1}$ (Figure 3). In comparison, on 28 July 2017, scattered clouds and a lower solar angle resulted in a maximum PAR of 1644 $\mu\text{mol m}^{-2} \text{s}^{-1}$, while the highest PAR on 1 October 2017 (autumn) only reached 1060 $\mu\text{mol m}^{-2} \text{s}^{-1}$. At the same time, the maximum respective air temperatures were 25.9 °C (8 June 2017), 26.5 °C (28 July 2017), and 18 °C (1 October 2017). A similar decreasing trend was also observed for VPD , with maximum values of ca. 2200 Pa reached in spring, 1500 Pa in summer, and 1000 Pa in autumn (Figure 3).

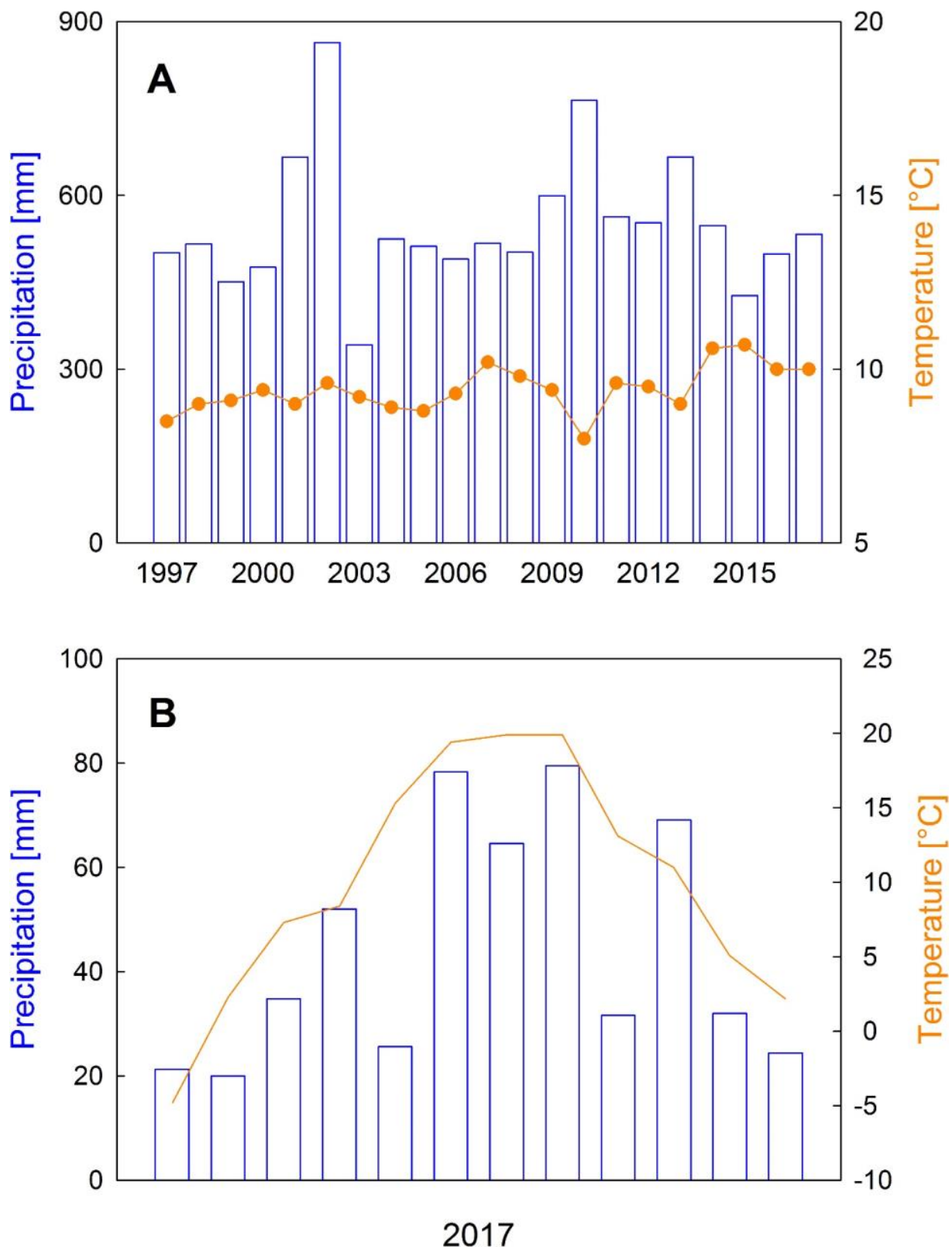


Figure 2. (A) Site climadiagram with annual average temperature and sum of precipitation for 1997–2017. (B) Monthly average temperature and sum of precipitation for 2017.

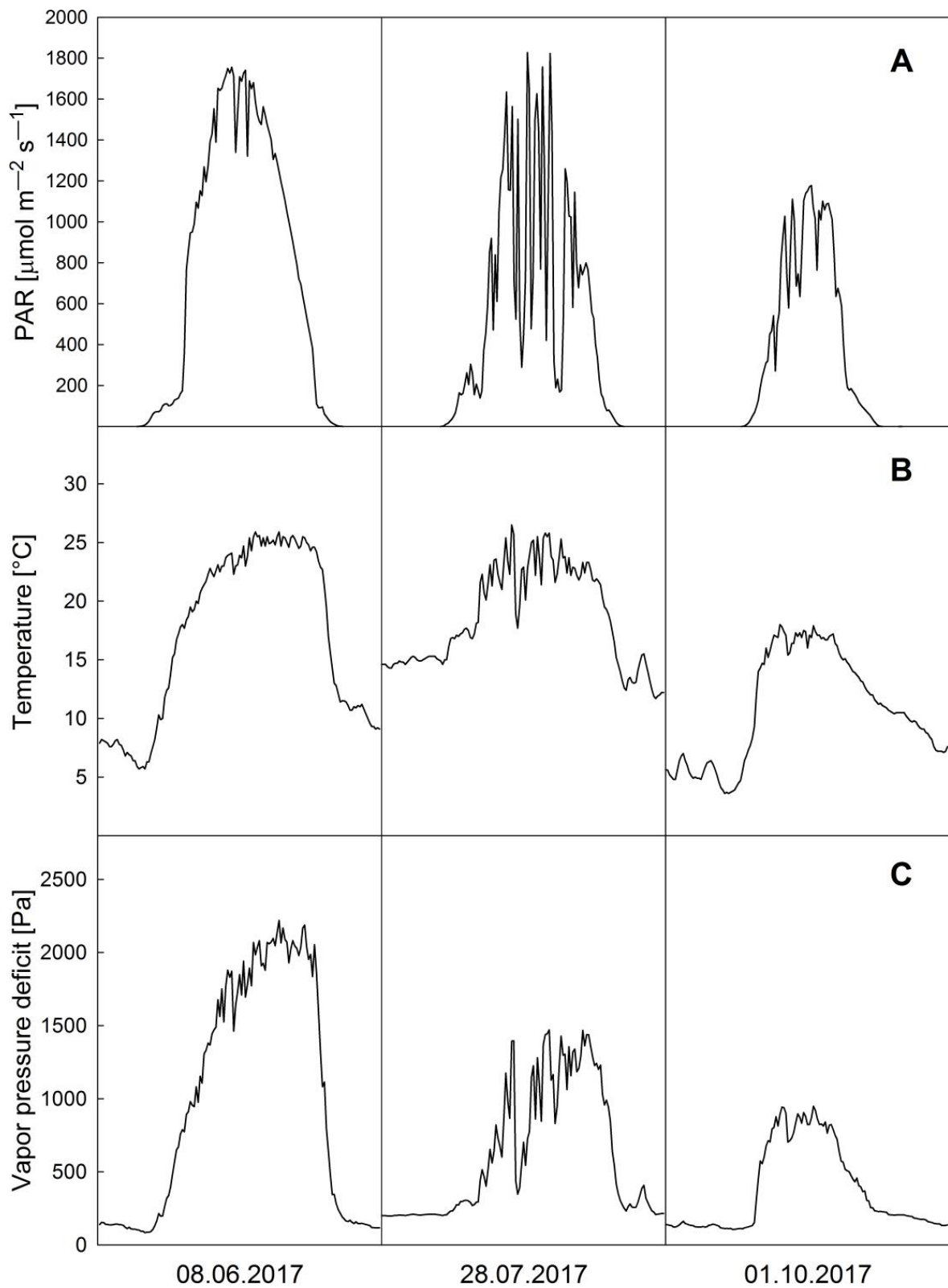


Figure 3. Daily trends in microclimatic parameters during measurement days. Global radiation ((A)—upper panel), air temperature ((B)—middle panel), and vapour pressure deficit ((C)—bottom panel) in spring, summer, and autumn (left to right).

3.2. Crown and Leaf Biometry

3.2.1. Crown Leaf Area and Projection

The greatest crown diameters were recorded in southerly, south-easterly, and south-westerly directions, reaching 3.4, 3.3, and 3.2 m, respectively, while the smallest crown diameters were recorded in easterly, north-easterly, and northern directions, at 2.3, 2.5, and 2.6 m, respectively (Figure 4A). The total area of leaves collected was 67.55 m², with 16.91 m² measured for northern leaves, 8.24 m² for eastern leaves, 29.05 m² for southern leaves, and 13.35 m² for western leaves (Figure 4B).

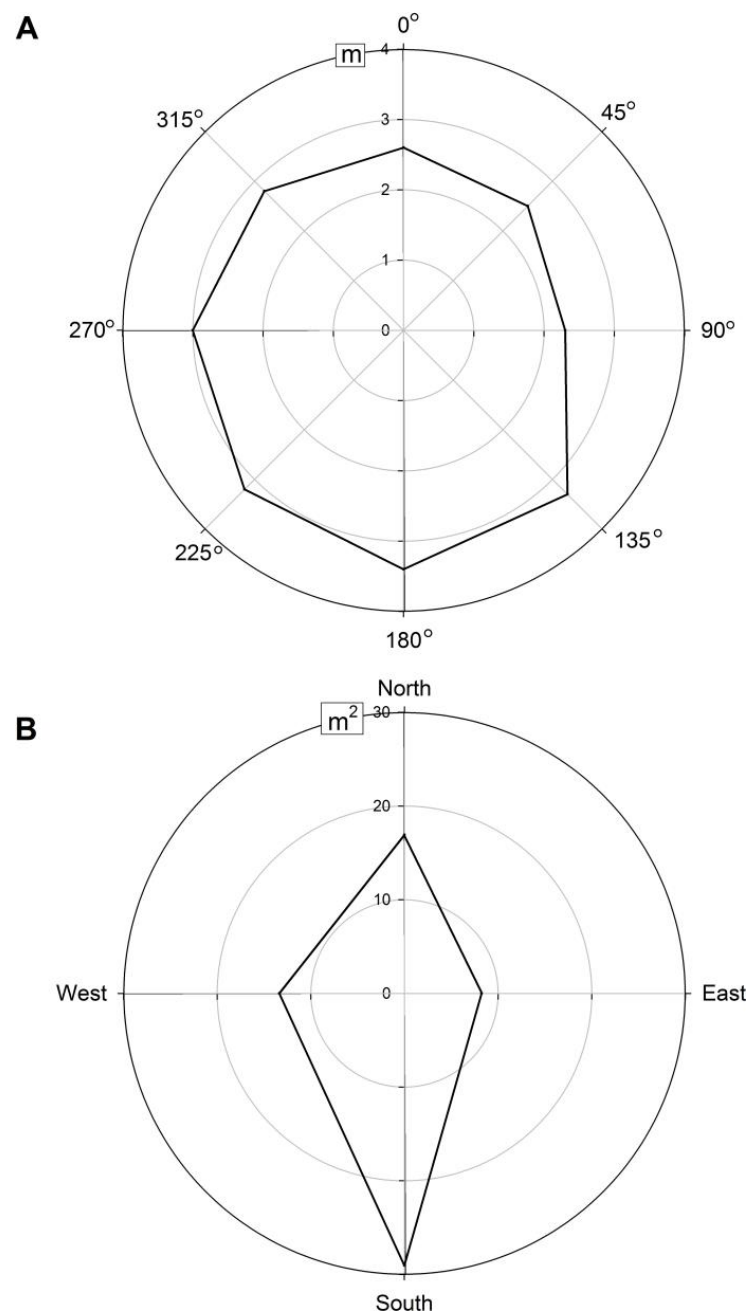


Figure 4. European Ash *F. excelsior* crown biometric parameters: distance projection represented in the horizontal angle from the north ((A)—upper panel) and scanned leaf area for the cardinal directions ((B)—bottom panel).

3.2.2. Leaf Biometry

LMA was highest in the east in both the upper and lower crown sections, with levels reaching 126 g m^{-2} , while the lowest *LMA* was observed in the west, reaching 98 g m^{-2} in the upper crown layer and 95 g m^{-2} in the lower layer (Figure 5).

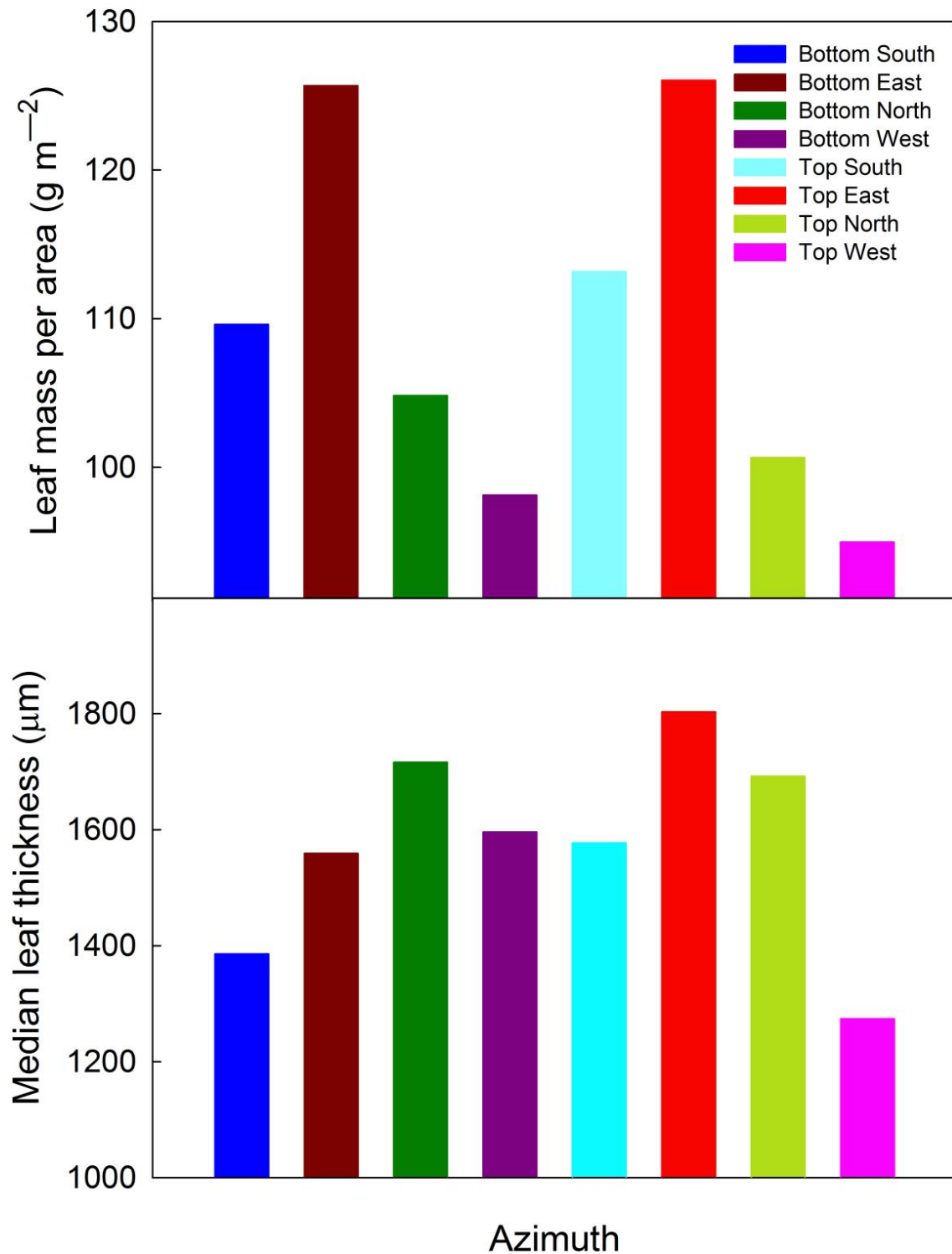


Figure 5. Leaf mass per area (upper panel) and median leaf thickness (bottom panel) in the four cardinal crown compartments.

Leaf thickness increased from the bottom of the crown compartment to the top in all cardinal directions except north, $p < 0.001$. Leaf thickness was lowest at the top of the western compartment (1274 μm) and highest at the top of the eastern compartment (1803 μm). Leaves in the southern compartment were significantly thinner than those in the north ($p < 0.05$).

3.3. Photosynthetic Activity

3.3.1. Maximum Rate of Photosynthesis

The highest P_{Nmax} was observed in the western (18.1 $\mu\text{mol}(\text{CO}_2) \text{m}^{-2} \text{s}^{-1}$) and southern (17.9 $\mu\text{mol}(\text{CO}_2) \text{m}^{-2} \text{s}^{-1}$) tree quadrants, while the lowest P_{Nmax} was recorded in the north (14.0 $\mu\text{mol}(\text{CO}_2) \text{m}^{-2} \text{s}^{-1}$) (Figure 6). The fitted light response indicated that light-saturated P_{Nmax} differed significantly between cardinal directions ($p < 0.001$), with high P_{Nmax} levels to the west and south differing significantly from those in the north (the eastern P_{Nmax} did not differ significantly from any other quadrant). The half-saturation constant KI did not differ significantly between quadrants ($p = 0.85$) (Table 1).

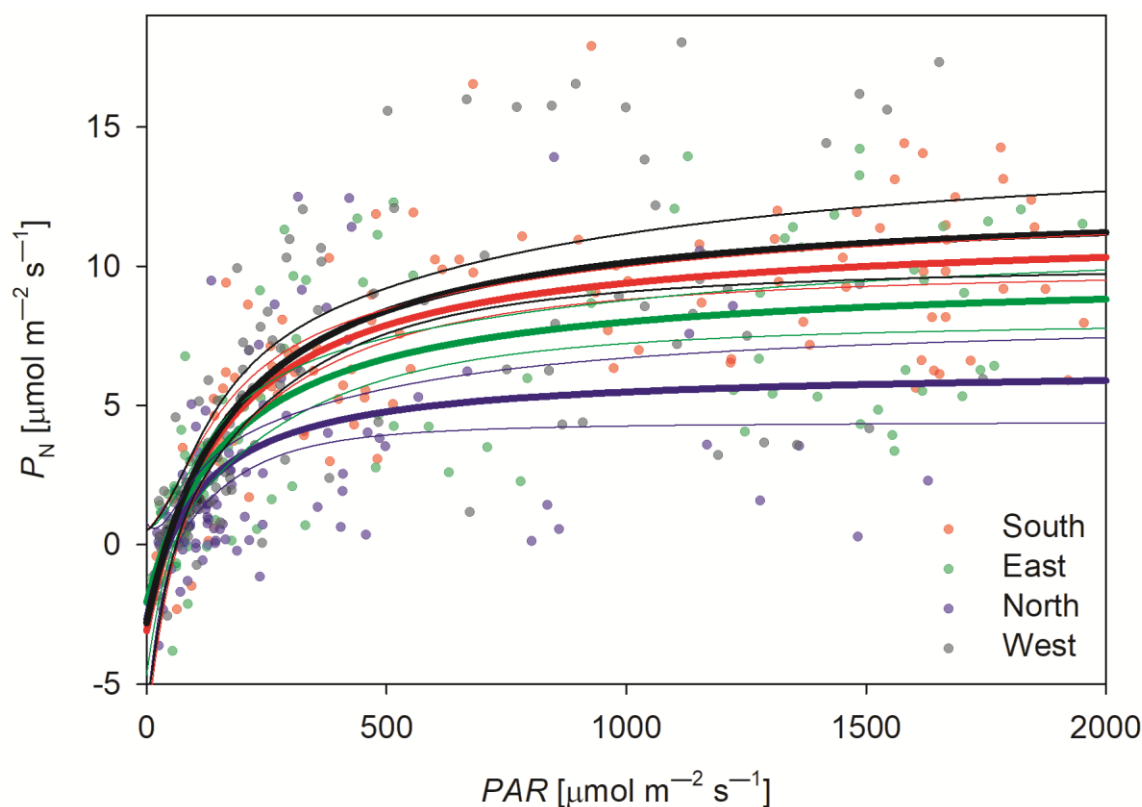


Figure 6. Dependence of net photosynthesis on photosynthetically active radiation. The thick lines are fitted response curves, and thin lines of the same colour indicate the respective confidence intervals.

Table 1. Light response curve coefficients for the four cardinal quadrants. Rd = dark respiration; $P_N \text{ max}$ = maximum modelled photosynthetic rate per individual; KI = half-saturation constant. Significant values are presented in bold.

	South			East			North			West		
	Coeff.	$\pm\text{SE}$	$p\text{-Value}$									
Rd	-3.08	1.81	0.09	-2.06	1.31	0.12	-2.68	1.74	0.13	-2.80	1.67	0.10
$P_N \text{ max}$	14.47	1.57	<0.0001	11.85	1.10	<0.0001	9.03	1.50	<0.0001	15.29	1.40	<0.0001
KI	159.58	55.96	0.01	176.34	75.27	0.02	105.98	63.88	0.10	182.43	73.81	0.02

3.3.2. Diurnal Trends in Photosynthesis and Photosynthetically Active Radiation

Daily P_N trends showed seasonal dynamics, with maxima reached during June–July and the lowest P_N levels recorded in October for all geographic quadrants (Figure 7). The highest P_N was recorded either before noon or in the afternoon in the eastern and southern quadrants, while the lowest values were recorded in the northern canopy compartment, irrespective of month or season. East-, south-, and west-facing leaves typically exhibit a unimodal P_N pattern, with a peak corresponding to the highest PAR (Figure 7). In contrast, north-facing leaves often showed a midday depression in P_N . While P_N was mostly positive during the day, it was negative throughout the day in the northern compartment during the autumn (due to low PAR), despite showing positive values in all other compartments.

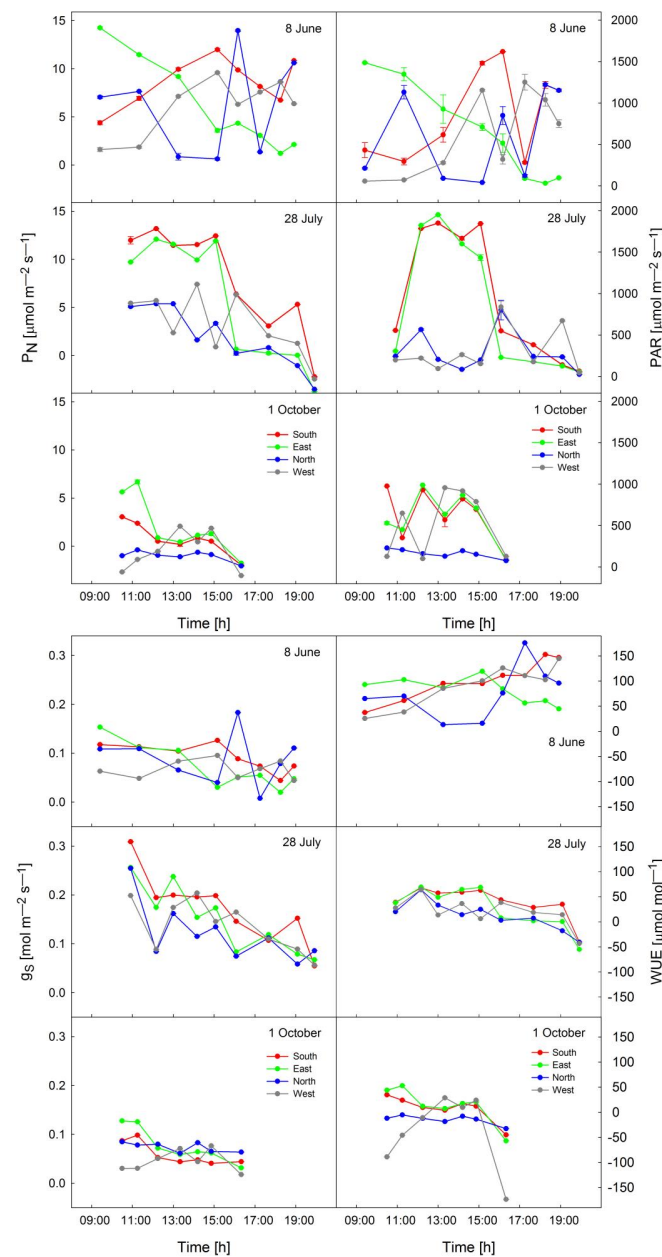


Figure 7. Diurnal variation in leaf gas exchange and illumination of crown compartments in three selected days. Top left panel—daily trends in net photosynthesis rate (P_N); top right panel—the illumination of the tree’s four cardinal quadrants (PAR); bottom left panel—daily trends in stomatal conductance (g_s); bottom right panel—daily trends in water use efficiency (WUE_i).

The highest leaf illumination in the eastern crown compartment occurred during the morning, after which it decreased constantly until nightfall (Figure 7). In the southern compartment, however, PAR increased until early afternoon, reaching over $1500 \mu\text{mol m}^{-2} \text{s}^{-1}$, while in the western compartment it increased constantly until evening, though it never exceeded $1500 \mu\text{mol m}^{-2} \text{s}^{-1}$. In the northern compartment, PAR displayed a bi-modal distribution, peaking in the morning and evening with a midday depression and only exceeding $1000 \mu\text{mol m}^{-2} \text{s}^{-1}$ in June. Maximum PAR occurred in June ($1711 \mu\text{mol m}^{-2} \text{s}^{-1}$) and the lowest in October ($1060 \mu\text{mol m}^{-2} \text{s}^{-1}$).

Unlike P_N and PAR , g_s was much more uniform throughout the tree crown, with most compartments reaching their highest levels in the morning (Figure 7). Later, as VPD increased, g_s declined in all crown compartments, with the exception of the western compartment in October, where g_s was low in the morning and peaked in the afternoon, probably due to low PAR and mutual shading by branches.

3.3.3. Water Use Efficiency

The $P_N:g_s$ relationship showed clear differences between compartments, with the highest P_N at a specific g_s occurring in the southern compartment and the lowest in the northern compartment, with eastern and western values somewhere between with no significant differences (Figure 7). While the initial phases of the curve slopes (g_s from $0-0.2 \text{ mol (H}_2\text{O) m}^{-2} \text{ s}^{-1}$) did not differ between cardinal quadrants ($p = 0.48$), the side intercepts of all quadrants showed a highly significant increase in P_N with increasing g_s ($p < 0.001$).

Water use efficiency WUE (Figure 7) was highest in June and lowest in October. WUE changed during the day, and it was usually highest in the specific crown compartment, which was illuminated by the highest PAR . Therefore, the lowest WUE was observed in the northern compartment. The most negative WUE during the season occurred in the west compartment in October in the morning and in the evening, as a result of the most negative P_N of all compartments.

3.3.4. Whole-Tree Photosynthesis

In all cases, the south-facing crown compartment contributed most to the total tree P_N (Table 2). In contrast, the contribution of the northern compartment was positive in June and July and negative in October. In spring, the total integrated daily sum of P_N per crown compartment was highest in the south, reaching $8556 \text{ mmol (CO}_2\text{) day}^{-1}$. While the contributions of all other segments were positive, the daily accumulated P_N in each of the other three segments only accounted for a maximum of 36% of southern P_N . Consequently, the southern crown compartment assimilated more CO_2 than all other segments combined. During summer, the ratio between P_N in the southern quadrant and the other quadrants was even greater than in spring, reaching 77%. P_N was lowest at the end of the vegetation season, with accumulated autumn P_N in the southern and eastern crown compartments positive but negative in the western and northern compartments (Table 2).

Table 2. Numerically integrated net photosynthesis (P_N ; $\text{mmol (CO}_2\text{) day}^{-1}$) for the four cardinal quadrants.

Measurement	South	East	North	West
Spring	8556 ± 125	2009 ± 26	3081 ± 74	2699 ± 41
Summer	7772 ± 43	1531 ± 12	1096 ± 36	1525 ± 9
Autumn	524 ± 22	394 ± 11	-369 ± 9	-84 ± 10

4. Discussion

Daily trends in *F. excelsior* P_N showed clear directionality, with the highest P_N occurring on the southern, eastern, and western sides and the lowest on the northern side. While light intensity appeared to be the main driver for differences in P_N with direction, it was

not the only factor. Our study demonstrated that foliage properties with respect to P_{Nmax} also differed between cardinal crown compartments, with light-saturated P_N lowest to the north and highest to the south and west (Figure 6). Also, P_N per unit g_s was lowest facing north and highest facing south (Figure 8). Overall, leaves were thin with low LMA in the western and southern quadrants, where P_N was high, and thickest in the eastern quadrant, where P_N and LMA were high (Figure 5).

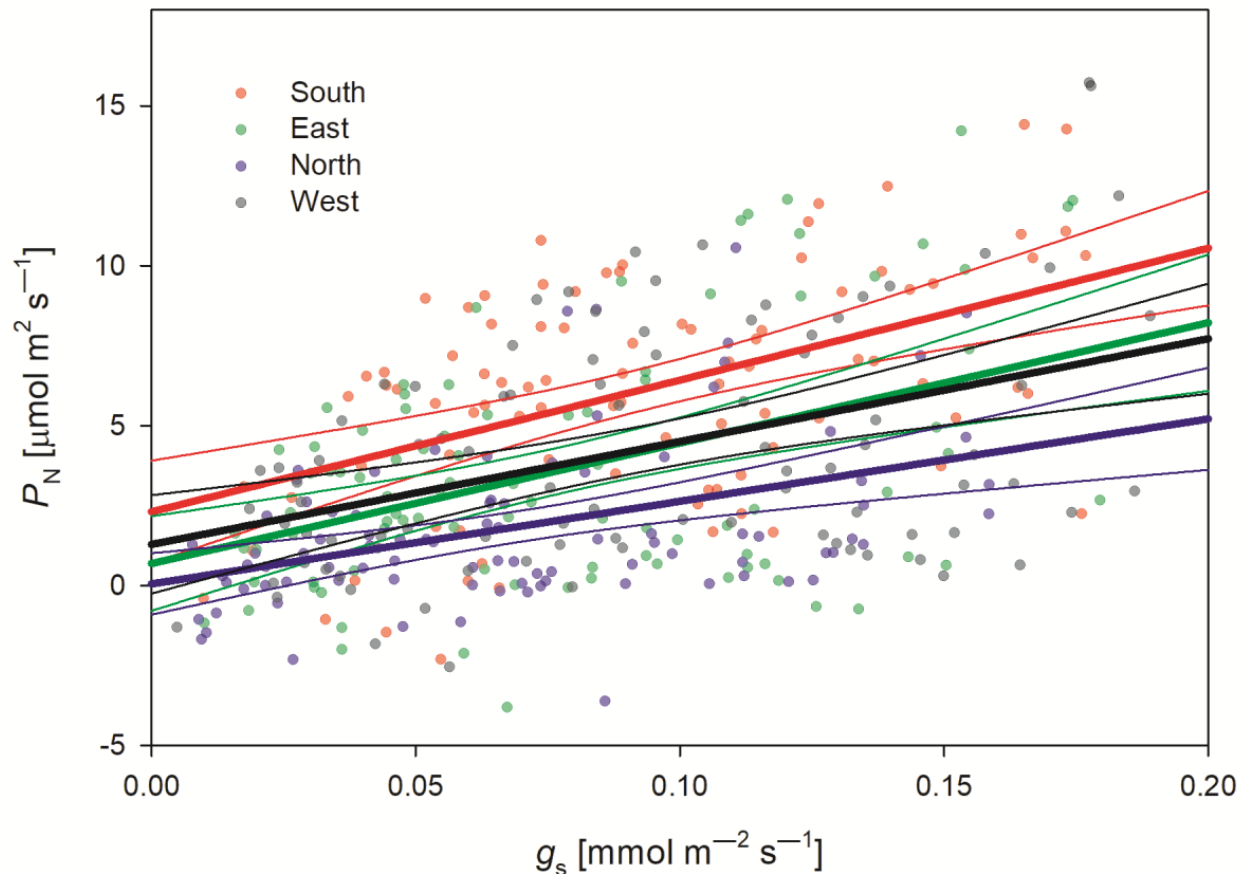


Figure 8. Relationship between net photosynthetic rate (P_N) and stomatal conductance (g_s) in June and July.

In our study, P_{Nmax} reached $18 \mu\text{mol} (\text{CO}_2) \text{m}^{-2} \text{s}^{-1}$, a value matching that reported for *F. excelsior* in a previous study [15], marking out *F. excelsior* as a species with a relatively high level of photosynthesis [12]. This high P_N corresponds with the species' high hydraulic conductance, resulting from its ring-porous anatomy, which in turn results in a high g_s [32]. A secondary reason for the high P_N , however, could have been the high fertility of the nitrogen-rich soil at the experimental site [30]. On the other hand, the observed light-saturated P_N was often lower than $18 \mu\text{mol} (\text{CO}_2) \text{m}^{-2} \text{s}^{-1}$ due to a high VPD (up to 3 kPa; Figure 3C), to which *F. excelsior* responded sensitively with a decline in stomatal conductance [32].

Maximum P_N values were usually recorded on those sides of the tree directly facing the sun at maximum illumination. As in [12], we recorded the highest P_N rates in June, when PAR was highest, and found no evidence for possible photoinhibition on the south-facing side of the crown. While we failed to observe a midday depression in P_N in June, there was a small midday depression in July and October (Figure 7). A similar midday photosynthesis depression in fully lit leaves in the southern crown compartment has also been reported for other broadleaf tree species, with Koike et al. [33], for example, reporting a midday decrease in P_{Nmax} during summer in the crown sub-layer of *F. mandshurica var. japonica*. In this case, the upper crown surface may have acted as a screen, reducing penetrating light to

a level optimal for sub-layer leaves. Einhorn [12], however, suggested that *F. excelsior* was relatively insensitive to photoinhibition when compared to European beech, *Fagus sylvatica*. A further reason for the midday depression in P_N may be associated with the increase in VPD , to which *F. excelsior* responds sensitively [32] by a decline in g_S [34,35]. In such cases, changes in g_S lead to a decrease in intercellular CO_2 concentration and a subsequent drop in Rubisco carboxylation efficiency [36]. Studies undertaken on broadleaf species over the last decade (e.g., ref. [37]) suggest that P_N could be limited not only by a midday decrease in g_S but also by leaf and stem water potential. For trees in warm environments, such as Mediterranean regions, and/or during hot summer events (heat waves), non-stomatal limitations may play a role in the midday depression of photosynthesis. Grassi et al. [38], however, suggested that this tends to be associated more with drought than radiation stress. In our case, the midday (13:00) depression in P_N rate observed in July in the southern canopy compartment correlated with a midday depression in g_S . On the other hand, g_S in July was roughly double that in June (Figure 7), suggesting that stomatal limitations imposed on photosynthesis were low. Consequently, we believe that the main reason for the midday decline in P_N was scattered PAR (Figure 3A) and the subsequent decline in energy available for photosynthesis.

The lowest P_N was always recorded in the northern crown compartment, irrespective of season, the main reason being the lack of PAR (Figure 7). On the other hand, we observed a midday depression in P_N in the northern compartment that was not the result of photoinhibition but rather caused by a decline in illumination. The biochemical properties of leaves may also have contributed to the low P_N in the northern compartment. For example, light response curves for photosynthesis data obtained in spring and summer indicated that, even in full light, P_{Nmax} was lower in the northern compartment (Figure 6), possibly due to a low maximum rate of carboxylation (V_{Cmax}) caused by poor nitrogen use efficiency in north-facing leaves [39]. At the same time, a low $P_N:g_S$ ratio was observed in the northern compartment across the whole g_S range (Figure 6), indicating poor intrinsic WUE . Similarly, Le Roux et al. (2001) [40] identified a steep WUE gradient in the crown leaves of an isolated English walnut (*Juglans regia*), with the lowest WUE in the north crown compartment. According to Gregoriou et al. (2007) [41], leaves that develop under low light reduce their stomatal density and g_S . In such cases, however, P_N declines even more due to differences in the leaves' internal structure, i.e., they have fewer palisade parenchyma. As the $P_N:g_S$ ratio was low at both low and high g_S levels in our study, we suggest large non-stomatal limitations to photosynthesis, probably as a result of low mesophyll conductance in the northern compartment [40,42,43]. Since mesophyll conductance increases with increasing PAR , reduced illumination during leaf development in the northern compartment may be one reason for the low intrinsic WUE [44]. However, instantaneous WUE , calculated from transpiration, will not be as low as the lower leaf temperatures in the northern compartment, which will result in a lower leaf VPD than leaves in the southern compartment.

For each crown compartment, leaf photosynthesis was lower in the early autumn than in July (see P_N in Figure 7), the decrease most likely attributable to changes during the early phases of leaf senescence, which is typically accompanied by altered g_S (Figure 7) and temperature-induced drought stress effects in leaves. It is now well established that the photosynthetic CO_2 fixation rate declines in broadleaf tree species with drought stress, i.e., whenever leaf water potential declines from 0 to a critical value of -2.0 to -3.0 MPa [45]. Moreover, photoperiod in the early autumn season appears to be one of the main driving factors decreasing photosynthesis in broadleaf tree species [46], caused by photoperiod- and temperature-dependent decreases in the maximum rate of CO_2 fixation by Rubisco and the rate of ribulose-bisphosphate regeneration [47].

In this study, LMA differed between *F. excelsior* crown compartments (Figure 5). According to Gregoriou et al. (2007) [41] and Escribano-Rocafort et al. (2017) [48], LMA reflects leaf traits related to leaf position and exposure to direct light, which vary most in crown positions. Leaf thickness, for example, increased from the bottom to the top of the crown, as also found by [49]. Importantly, leaf thickness (Table 1) did not correlate perfectly

with *LMA* when the thickest leaves were in question. Furthermore, the highest *LMA* was found in the northern compartment, and the thinnest leaves were found in the south. The combination of leaf thickness and *LMA* provides an estimate of leaf internal density, which affects mesophyll conductance to CO_2 [42,43], with low density suggesting a low P_N [50]. A low conductance for CO_2 resulting from the difference in leaf structure in the north may be one reason for the low *WUE* in this cardinal quadrant. Furthermore, the high density of thin leaves in the south-facing crown compartment may be related to a higher level of drought stress in these leaves than in the northern quadrant [51].

The total contribution of each cardinal quadrant to the total tree P_N results from the combination of leaf area, illumination levels, and the biochemical properties of the leaves in each compartment. When we integrated P_N over a whole day (Table 2), the highest P_N was recorded in the east- and south-facing crown compartments. Though the south received the highest illumination levels, P_N may already have been constrained by a high *VPD* at midday (Figure 3C). *VPD* will also be the main factor limiting P_N in the western compartment compared with the east [52]. The contribution of the northern quadrant to total tree P_N varied greatly throughout the monitoring period, with the distribution of P_N being bimodal in the spring and summer when the northern compartment received solar radiation in the morning and evening. As the days became shorter in the autumn, however, mutual shading by branches caused respiration to prevail over carbon assimilation. As a result, P_N in October was negative all day in north-facing leaves, while the other cardinal quadrants all yielded a positive P_N (Figure 7). Consequently, semi-solitary trees develop an asymmetric foliage distribution, with the largest leaf area in the south-facing quadrant. This high leaf area, combined with the highest illumination and high P_{Nmax} , means that >50% of all carbon was assimilated in the south-facing quadrant and <50% in the other three quadrants combined (Table 2). Two questions receiving little attention to date are how carbon assimilated predominantly in the southern compartment redistributes to the shaded parts of the crown and how water for transpiration redistributes from shaded to sunlit parts of the tree following the gradient of water potentials [53]. On a whole tree scale, roots and the crown are functionally connected, and aboveground asymmetry often correlates with asymmetry belowground [54]. Manipulative experiments on seedlings suggest that carbohydrates from a specific crown compartment predominantly support the same compartment below ground [55]. Consequently, future research could be directed towards assessing how asymmetry in carbohydrate production translates to asymmetry in the root system.

5. Conclusions

In this paper, the differences in P_N in different cardinal crown quadrants of a semi-solitary *F. excelsior* were described. We found that south-facing foliage contributed most to overall tree P_N , with most of the difference attributable to the intensity of illumination. However, the leaves also differed in P_{Nmax} under saturated light, suggesting a difference in biochemical limits for photosynthesis. The difference in P_{Nmax} was also associated with differences in intrinsic *WUE*. The southern crown compartment also contributed most to total tree carbon assimilation, which was exacerbated by the southern quadrant also having the largest leaf area. Future research employing larger tree datasets than those used in the present study will be needed to generalise these findings. Based on our findings, we suggest a need for standardising the selection of leaves when measuring P_N in mature trees to capture spatial variability within the canopy. Any extrapolation of single-leaf measurements to whole-tree and canopy levels should be accompanied by a detailed study of leaf area distribution.

Author Contributions: Conceptualisation, J.Č., J.U. and M.B.; methodology, R.S.M., J.U., J.W. and M.B.; software, J.U.; validation, R.S.M., M.B. and J.U.; formal analysis, R.S.M., J.W. and J.Č.; investigation, J.Č., J.U. and M.B.; resources, R.S.M., M.B., J.W. and J.Č.; data curation, M.B., J.U. and R.S.M.; writing—original draft preparation, J.Č., M.B. and R.S.M.; writing—review and editing, R.S.M. and J.U.; visualisation, J.U.; supervision, J.Č., M.B. and J.U.; project administration, R.S.M. and J.Č.;

funding acquisition, J.Č., J.W., M.B. and R.S.M. All authors have read and agreed to the published version of the manuscript.

Funding: This research was performed as part of a project of the Internal Grant Agency of the Faculty of Forestry and Wood Technology (No.: LDF_VP_2019042) and project No. 21-11487S of the Czech Science Foundation. Leaf biometric characteristics were measured with the aid of ECOPOLARIS infrastructure, provided under Project No. CZ.02.1.01/0.0/0.0/16_013/0001708 of the Czech Ministry of Education, Youth, and Sports. VUKOZ participation was supported through institutional support from the Department of Phytoenergy (VUKOZ-IP-00027073).

Data Availability Statement: The raw data supporting the conclusions of this article will be made available by the authors upon request on the address robert.majewski@mendelu.cz.

Acknowledgments: The authors are grateful to Kevin Roche for English revision.

Conflicts of Interest: The author declares no conflicts of interest.

References

- Ryu, Y.; Berry, J.A.; Baldocchi, D.D. What Is Global Photosynthesis? History, Uncertainties and Opportunities. *Remote Sens. Environ.* **2019**, *223*, 95–114. [[CrossRef](#)]
- Baslam, M.; Mitsui, T.; Hodges, M.; Priesack, E.; Herritt, M.T.; Aranjuelo, I.; Sanz-Sáez, Á. Photosynthesis in a Changing Global Climate: Scaling Up and Scaling Down in Crops. *Front. Plant Sci.* **2020**, *11*, 882. [[CrossRef](#)]
- De Pury, D.G.G.; Farquhar, G.D. Simple Scaling of Photosynthesis from Leaves to Canopies without the Errors of Big-leaf Models. *Plant Cell Environ.* **1997**, *20*, 537–557. [[CrossRef](#)]
- Strigul, N. Individual-Based Models and Scaling Methods for Ecological Forestry: Implications of Tree Phenotypic Plasticity. In *Sustainable Forest Management*; InTech: Rijeka, Croatia, 2012; pp. 359–384.
- Parker, G.G.; Harmon, M.E.; Lefsky, M.A.; Chen, J.; Pelt, R.V.; Weis, S.B.; Thomas, S.C.; Winner, W.E.; Shaw, D.C.; Frankling, J.F. Three-Dimensional Structure of an Old-Growth Pseudotsuga-Tsuga Canopy and Its Implications for Radiation Balance, Microclimate, and Gas Exchange. *Ecosystems* **2004**, *7*, 440–453. [[CrossRef](#)]
- Yang, W.-W.; Chen, X.-L.; Saudreau, M.; Zhang, X.-Y.; Zhang, M.-R.; Liu, H.-K.; Costes, E.; Han, M.-Y. Canopy Structure and Light Interception Partitioning among Shoots Estimated from Virtual Trees: Comparison between Apple Cultivars Grown on Different Interstocks on the Chinese Loess Plateau. *Trees* **2016**, *30*, 1723–1734. [[CrossRef](#)]
- Yang, W.; Ma, X.; Ma, D.; Shi, J.; Hussain, S.; Han, M.; Costes, E.; Zhang, D. Modeling Canopy Photosynthesis and Light Interception Partitioning among Shoots in Bi-Axis and Single-Axis Apple Trees (*Malus Domestica* Borkh). *Trees* **2021**, *35*, 845–861. [[CrossRef](#)]
- Escribano-Rocafort, A.G.; Ventre-Lespiaucq, A.B.; Granado-Yela, C.; Rubio De Casas, R.; Delgado, J.A.; Balaguer, L. The Expression of Light-Related Leaf Functional Traits Depends on the Location of Individual Leaves within the Crown of Isolated *Olea Europaea* Trees. *Ann. Bot.* **2016**, *117*, 643–651. [[CrossRef](#)]
- Granado-Yela, C.; García-Verdugo, C.; Carrillo, K.; Rubio De Casas, R.; Kleczkowski, L.A.; Balaguer, L. Temporal Matching among Diurnal Photosynthetic Patterns within the Crown of the Evergreen Sclerophyll *Olea europaea* L. *Plant Cell Environ.* **2011**, *34*, 800–810. [[CrossRef](#)]
- Sinoquet, H.; Le Roux, X.; Adam, B.; Ameglio, T.; Daudet, F.A. RATP: A Model for Simulating the Spatial Distribution of Radiation Absorption, Transpiration and Photosynthesis within Canopies: Application to an Isolated Tree Crown. *Plant Cell Environ.* **2001**, *24*, 395–406. [[CrossRef](#)]
- Peltier, J.-P.; Marigo, G. Drought Adaptation in *Fraxinus Excelsior* L.: Physiological Basis of the Elastic Adjustment. *J. Plant Physiol.* **1999**, *154*, 529–535. [[CrossRef](#)]
- Einhorn, K.S. Growth and Photosynthesis of Ash *Fraxinus Excelsior* and Beech *Fagus Sylvatica* Seedlings in Response to a Light Gradient Following Natural Gap Formation. *Ecol. Bull.* **2007**, *52*, 147–165.
- Van Der Tol, C.; Dolman, A.J.; Waterloo, M.J.; Raspor, K. Topography Induced Spatial Variations in Diurnal Cycles of Assimilation and Latent Heat of Mediterranean Forest. *Biogeosciences* **2007**, *4*, 137–154. [[CrossRef](#)]
- Hommel, R.; Siegwolf, R.; Saurer, M.; Farquhar, G.D.; Kayler, Z.; Ferrio, J.P.; Gessler, A. Drought Response of Mesophyll Conductance in Forest Understory Species—Impacts on Water-Use Efficiency and Interactions with Leaf Water Movement. *Physiol. Plant.* **2014**, *152*, 98–114. [[CrossRef](#)]
- Zhou, S.; Medlyn, B.; Sabaté, S.; Sperlich, D.; Prentice, I.C.; Whitehead, D. Short-Term Water Stress Impacts on Stomatal, Mesophyll and Biochemical Limitations to Photosynthesis Differ Consistently among Tree Species from Contrasting Climates. *Tree Physiol.* **2014**, *34*, 1035–1046. [[CrossRef](#)]
- Li, S.; Feifel, M.; Karimi, Z.; Schuldt, B.; Choat, B.; Jansen, S. Leaf Gas Exchange Performance and the Lethal Water Potential of Five European Species during Drought. *Tree Physiol.* **2015**, *36*, tpe117. [[CrossRef](#)]
- Premachandra, G.S.; Chaney, W.R.; Holt, H.A. Gas Exchange and Water Relations of *Fraxinus Americana* Affected by Flurprimidol. *Tree Physiol.* **1997**, *17*, 97–103. [[CrossRef](#)]

18. Zhang, S.Y.; Zhang, G.C.; Liu, X.; Xia, J.B. The Responses of Photosynthetic Rate and Stomatal Conductance of Fraxinus Rhynchophylla to Differences in CO₂ Concentration and Soil Moisture. *Photosynthetica* **2013**, *51*, 359–369. [CrossRef]
19. Flower, C.; Lynch, D.; Knight, K.; Gonzalez-Meler, M. Biotic and Abiotic Drivers of Sap Flux in Mature Green Ash Trees (*Fraxinus pennsylvanica*) Experiencing Varying Levels of Emerald Ash Borer (*Agrilus planipennis*) Infestation. *Forests* **2018**, *9*, 301. [CrossRef]
20. Lichtenthaler, H.K.; Babani, F.; Navrátil, M.; Buschmann, C. Chlorophyll Fluorescence Kinetics, Photosynthetic Activity, and Pigment Composition of Blue-Shade and Half-Shade Leaves as Compared to Sun and Shade Leaves of Different Trees. *Photosynth. Res.* **2013**, *117*, 355–366. [CrossRef]
21. Fini, A.; Guidi, L.; Giordano, C.; Baratto, M.C.; Ferrini, F.; Brunetti, C.; Calamai, L.; Tattini, M. Salinity Stress Constrains Photosynthesis in Fraxinus Ornus More When Growing in Partial Shading than in Full Sunlight: Consequences for the Antioxidant Defence System. *Ann. Bot.* **2014**, *114*, 525–538. [CrossRef]
22. Rubio De Casas, R.; Vargas, P.; Pérez-Corona, E.; Manrique, E.; Quintana, J.R.; García-Verdugo, C.; Balaguer, L. Field Patterns of Leaf Plasticity in Adults of the Long-Lived Evergreen Quercus Coccifera. *Ann. Bot.* **2007**, *100*, 325–334. [CrossRef] [PubMed]
23. Wyka, T.P.; Oleksyn, J.; Żytkowiak, R.; Karolewski, P.; Jagodziński, A.M.; Reich, P.B. Responses of Leaf Structure and Photosynthetic Properties to Intra-Canopy Light Gradients: A Common Garden Test with Four Broadleaf Deciduous Angiosperm and Seven Evergreen Conifer Tree Species. *Oecologia* **2012**, *170*, 11–24. [CrossRef] [PubMed]
24. Valladares, F.; Niinemets, Ü. Shade Tolerance, a Key Plant Feature of Complex Nature and Consequences. *Annu. Rev. Ecol. Evol. Syst.* **2008**, *39*, 237–257. [CrossRef]
25. Kalapos, T.; Csontos, P. Variation in Leaf Structure and Function of the Mediterranean Tree *Fraxinus Ornus* L. Growing in Ecologically Contrasting Habitats at the Margin of Its Range. *Plant Biosyst. Int. J. Deal. Asp. Plant Biol.* **2003**, *137*, 73–82. [CrossRef]
26. Bartlett, G.A.; Remphrey, W.R. The Effect of Reduced Quantities of Photosynthetically Active Radiation on *Fraxinus Pennsylvanica* Growth and Architecture. *Can. J. Bot.* **1998**, *76*, 1359–1365. [CrossRef]
27. Niinemets, Ü. A Review of Light Interception in Plant Stands from Leaf to Canopy in Different Plant Functional Types and in Species with Varying Shade Tolerance. *Ecol. Res.* **2010**, *25*, 693–714. [CrossRef]
28. Monteith, J.L.; Unsworth, M.H. *Principles of Environmental Physics*; Academic Press: Kidlington, UK, 2013; ISBN 9780123869104.
29. IUSS Working Group WRB. *World Reference Base for Soil Resources 2014. International Soil Classification System for Naming Soils and Creating Legends for Soil Maps*; FAO: Rome, Italy, 2014; Available online: <https://www.fao.org/3/i3794en/I3794en.pdf> (accessed on 10 March 2024).
30. Majewski, R.S.; Valenta, J.; Tábořík, P.; Weger, J.; Kučera, A.; Patočka, Z.; Čermák, J. Geophysical Imaging of Tree Root Absorption and Conduction Zones under Field Conditions: A Comparison of Common Geoelectrical Methods. *Plant Soil* **2022**, *481*, 447–473. [CrossRef]
31. Smyth, G.K. *Numerical Integration*; Wiley: Hoboken, NJ, USA, 1998; pp. 3088–3095.
32. Stohr, A.; Losch, R. Xylem Sap Flow and Drought Stress of Fraxinus Excelsior Saplings. *Tree Physiol.* **2004**, *24*, 169–180. [CrossRef]
33. Koike, T.; Kitaoka, S.; Ichie, T.; Lei, T.T.; Kitao, M. Photosynthetic Characteristics of Mixed Deciduous-Broadleaf Forests from Leaf to Stand. *Glob. Environ. Chang. Ocean Land Tokyo Terrapub* **2004**, 453–472.
34. Pathre, U.; Sinha, A.K.; Shirke, P.A.; Sane, P.V. Factors Determining the Midday Depression of Photosynthesis in Trees under Monsoon Climate. *Trees* **1998**, *12*, 472. [CrossRef]
35. Kamakura, M.; Kosugi, Y.; Takanashi, S.; Matsumoto, K.; Okumura, M.; Philip, E. Patchy Stomatal Behavior during Midday Depression of Leaf CO₂ Exchange in Tropical Trees. *Tree Physiol.* **2011**, *31*, 160–168. [CrossRef] [PubMed]
36. Muraoka, H.; Tang, Y.; Terashima, I.; Koizumi, H.; Washitani, I. Contributions of Diffusional Limitation, Photoinhibition and Photorespiration to Midday Depression of Photosynthesis in *Arisaema Heterophyllum* in Natural High Light. *Plant Cell Environ.* **2000**, *23*, 235–250. [CrossRef]
37. Zhang, Y.; Meinzer, F.C.; Qi, J.; Goldstein, G.; Cao, K. Midday Stomatal Conductance Is More Related to Stem Rather than Leaf Water Status in Subtropical Deciduous and Evergreen Broadleaf Trees. *Plant Cell Environ.* **2013**, *36*, 149–158. [CrossRef] [PubMed]
38. Grassi, G.; Ripullone, F.; Borghetti, M.; Raddi, S.; Magnani, F. Contribution of Diffusional and Non-Diffusional Limitations to Midday Depression of Photosynthesis in *Arbutus unedo* L. *Trees* **2009**, *23*, 1149–1161. [CrossRef]
39. Iio, A.; Fukasawa, H.; Nose, Y.; Kato, S.; Kakubari, Y. Vertical, Horizontal and Azimuthal Variations in Leaf Photosynthetic Characteristics within a Fagus Crenata Crown in Relation to Light Acclimation. *Tree Physiol.* **2005**, *25*, 533–544. [CrossRef] [PubMed]
40. Le Roux, X.; Bariac, T.; Sinoquet, H.; Genty, B.; Piel, C.; Mariotti, A.; Girardin, C.; Richard, P. Spatial Distribution of Leaf Water-use Efficiency and Carbon Isotope Discrimination within an Isolated Tree Crown. *Plant Cell Environ.* **2001**, *24*, 1021–1032. [CrossRef]
41. Gregoriou, K.; Pontikis, K.; Vemmos, S. Effects of Reduced Irradiance on Leaf Morphology, Photosynthetic Capacity, and Fruit Yield in Olive (*Olea europaea* L.). *Photosynthetica* **2007**, *45*, 172–181. [CrossRef]
42. Flexas, J.; Bota, J.; Loreto, F.; Cornic, G.; Sharkey, T.D. Diffusive and Metabolic Limitations to Photosynthesis under Drought and Salinity in C₃ Plants. *Plant Biol.* **2004**, *6*, 269–279. [CrossRef]
43. Flexas, J.; Barbour, M.M.; Brendel, O.; Cabrera, H.M.; Carriqui, M.; Díaz-Espejo, A.; Douthe, C.; Dreyer, E.; Ferrio, J.P.; Gago, J.; et al. Mesophyll Diffusion Conductance to CO₂: An Unappreciated Central Player in Photosynthesis. *Plant Sci.* **2012**, *193–194*, 70–84. [CrossRef]
44. Xiong, D.; Douthe, C.; Flexas, J. Differential Coordination of Stomatal Conductance, Mesophyll Conductance, and Leaf Hydraulic Conductance in Response to Changing Light across Species. *Plant Cell Environ.* **2018**, *41*, 436–450. [CrossRef]

45. Ni, B.-R.; Pallardy, S.G. Response of Gas Exchange to Water Stress in Seedlings of Woody Angiosperms. *Tree Physiol.* **1991**, *8*, 1–9. [[CrossRef](#)] [[PubMed](#)]
46. Yu, H.; Zhou, G.; Lv, X.; He, Q.; Zhou, M. Stomatal Limitation Is Able to Modulate Leaf Coloration Onset of Temperate Deciduous Tree. *Forests* **2022**, *13*, 1099. [[CrossRef](#)]
47. Kinoshita, T.; Kume, A.; Hanba, Y.T. Seasonal Variations in Photosynthetic Functions of the Urban Landscape Tree Species Ginkgo Biloba: Photoperiod Is a Key Trait. *Trees* **2021**, *35*, 273–285. [[CrossRef](#)]
48. Escribano-Rocafort, A.G.; Ventre-Lespiaucq, A.B.; Granado-Yela, C.; Rubio De Casas, R.; Delgado, J.A.; Escudero, A.; Balaguer, L. Intraindividual Variation in Light-Related Functional Traits: Magnitude and Structure of Leaf Trait Variability across Global Scales in Olea Europaea Trees. *Trees* **2017**, *31*, 1505–1517. [[CrossRef](#)]
49. Gebauer, R.; Volarik, D.; Urban, J.; Borja, I.; Nagy, N.E.; Eldhuset, T.D.; Krokene, P. Effect of Thinning on Anatomical Adaptations of Norway Spruce Needles. *Tree Physiol.* **2011**, *31*, 1103–1113. [[CrossRef](#)] [[PubMed](#)]
50. Niinemets, Ü. Research Review. Components of Leaf Dry Mass per Area—Thickness and Density—Alter Leaf Photosynthetic Capacity in Reverse Directions in Woody Plants. *New Phytol.* **1999**, *144*, 35–47. [[CrossRef](#)]
51. Nardini, A. Hard and Tough: The Coordination between Leaf Mechanical Resistance and Drought Tolerance. *Flora* **2022**, *288*, 152023. [[CrossRef](#)]
52. Ishida, A.; Toma, T. Marjenah Leaf Gas Exchange and Chlorophyll Fluorescence in Relation to Leaf Angle, Azimuth, and Canopy Position in the Tropical Pioneer Tree, Macaranga Conifera. *Tree Physiol.* **1999**, *19*, 117–124. [[CrossRef](#)]
53. Šenfeldr, M.; Urban, J.; Maděra, P.; Kučera, J. Redistribution of Water via Layering Branches between Connected Parent and Daughter Trees in Norway Spruce Clonal Groups. *Trees Struct. Funct.* **2015**, *30*, 5–17. [[CrossRef](#)]
54. Wang, H.; Qin, J.; Hu, Y.; Guo, C. Asymmetric Growth of Belowground and Aboveground Tree Organs and Their Architectural Relationships: A Review. *Can. J. For. Res.* **2023**, *53*, 315–327. [[CrossRef](#)]
55. Dong, T.; Duan, B.; Korpelainen, H.; Niinemets, Ü.; Li, C. Asymmetric Pruning Reveals How Organ Connectivity Alters the Functional Balance between Leaves and Roots of Chinese Fir. *J. Exp. Bot.* **2019**, *70*, 1941–1953. [[CrossRef](#)] [[PubMed](#)]

Disclaimer/Publisher’s Note: The statements, opinions and data contained in all publications are solely those of the individual author(s) and contributor(s) and not of MDPI and/or the editor(s). MDPI and/or the editor(s) disclaim responsibility for any injury to people or property resulting from any ideas, methods, instructions or products referred to in the content.